Available online at www.eccomasproceedia.org
Eccomas Proceedia COMPDYN (2017) 3235-3247

ECCOMAS
Proceedia

COMPDYN 2017
6th ECCOMAS Thematic Conference on
Computational Methods in Structural Dynamics and Earthquake Engineering
M. Papadrakakis, M. Fragiadakis (eds.)
Rhodes Island, Greece, 15–17 June 2017

USING AN INSTRUMENTED VEHICLE TO ESTIMATE SURFACE ROUGHNESS OF A BRIDGE

Ying Zhan, Francis T. K. Au

The University of Hong Kong
The University of Hong Kong, Pokfulam, Hong Kong
{yingzhan, francis.au}@hku.hk

Keywords: Finite Element Modeling, Parameter Identification, Roughness Profile, Vehicle Bridge Interaction.

Abstract. *Bridge parameter identification based on vehicle-bridge interaction theory and data extracted from the vehicle response has many potential applications. However, its real application is restricted, partly due to the bridge surface roughness, which can significantly contaminate the vehicle response data and make parameter identification hard or even impossible. If the bridge surface roughness can be detected with satisfactory accuracy, then it is possible to eliminate its uncertain effect on the vehicle-bridge interaction, which will facilitate more accurate identification. This study aims to provide a way to estimate the surface roughness profile of a bridge using the acceleration data gathered from a vehicle running on the bridge twice with different masses. The mass-spring-damper model is used to simulate the moving vehicle. Finite element simulation results show that this method is able to estimate the surface roughness profile accurately.*

Peer-review under responsibility of the organizing committee of COMPDYN 2017.
doi: 10.7712/120117.5641.17737

1 INTRODUCTION

Parameter identification is useful for estimating the dynamic properties of newly built bridges, detecting damage in existing bridges, and assessing the serviceability of old bridges. Various methods have been proposed for identifying various bridge parameters. One of the economical and convenient methods is the drive-by parameter identification approach.

The bridge and the vehicle running on can be considered as a coupled vibration system. The properties of a moving vehicle can be identified from the bridge vibration data [1]. Similarly, the bridge dynamic parameters can also be derived from the vibration data measured from an instrumented vehicle moving on a bridge [2, 3].

Using vehicles instrumented with sensors to detect bridge parameters is an indirect method that is both economical and convenient, and the disruption to normal traffic on the bridge can be minimized as compared to other methods [4]. However, this method is prone to environmental and other types of noise. In particular, the presence of surface roughness of the bridge can seriously affect the vehicle-bridge interaction phenomenon and contaminate the vehicle vibration data. Most of the theoretical research work has ignored the surface roughness. Some used simple waves to simulate the surface roughness, such as sinusoidal wave [5]; or considered in the vehicle-bridge interaction simulation but with an impractically small magnitude [6]. These methods are therefore incapable of dealing with real surface roughness. As a result, most of the experiments in related fields were conducted on bridge models with smooth surface in lab environment [7].

There were studies on road roughness detection with promising results, but their target and focus are different from those in this study. Their focus was on the statistical properties of road roughness, such as power spectral density, which is usually used for classification of road quality based on standards such as ISO 8608. This study, on the other hand, focuses on the estimation of surface roughness profile, which is useful in eliminating its uncertain effect on the vehicle-bridge interaction system.

2 THEORY

The vehicle-bridge interaction model with smooth surface is first examined, followed by another model with surface roughness. A method for estimating surface roughness profile is proposed accordingly based on the latter model.

2.1 Vehicle-bridge interaction dynamics for a smooth bridge

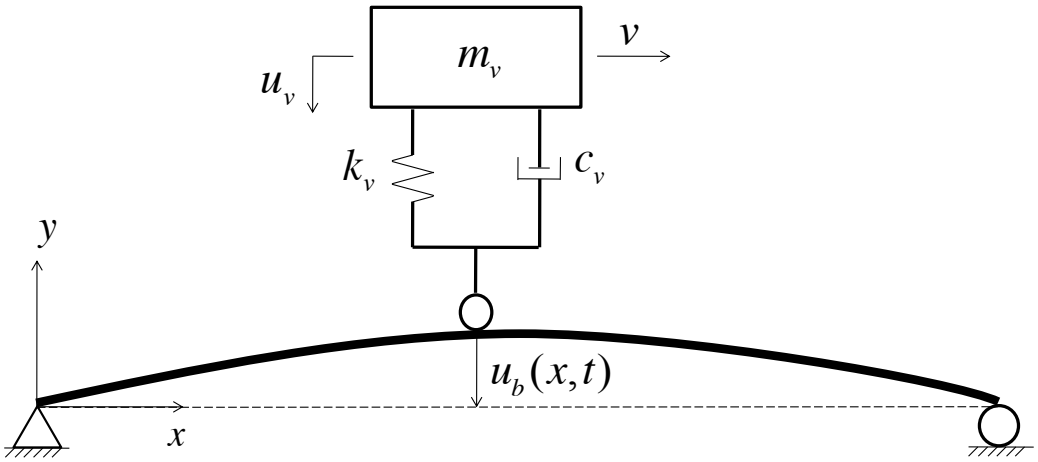

Figure 1: Vehicle-bridge interaction model

A vehicle is traveling on a simply supported uniform bridge with smooth surface as shown in Figure 1. The vehicle is modeled as a mass-spring-damper model, which captures the main features of the vehicle and is relatively simple to analyze. For this vehicle-bridge interaction system without surface roughness, the equation of motion of the bridge can be written as

$$\overline{m}\frac{\partial^2 u_b(x,t)}{\partial t^2}+c\frac{\partial u_b(x,t)}{\partial t}+EI\frac{\partial^4 u_b(x,t)}{\partial x^4}=F_c(t)\delta(x-vt) \tag{1}$$

where $\overline{m}$, c, E and I denote the mass per unit length, damping, elastic modulus and moment of inertia of the beam, respectively; $u_b(x,t)$ is the vertical displacement of the bridge at abscissa x and time t; $F_c(t)$ is the contact force between the vehicle and bridge; v is the speed of vehicle; and $\delta(x-vt)$ is the Dirac delta function to describe the movement of vehicle on the bridge mathematically, i.e.

$$\delta(x)=\begin{cases}+\infty, & x=0\\ 0, & x\neq 0\end{cases} \quad \text{and} \quad \int_{-\infty}^{+\infty}\delta(x)dx=1 \tag{2}$$

The equation of motion of the vehicle can be written as

$$m_v\frac{d^2u_v(t)}{dt^2}+c_v\left[\frac{du_v(t)}{dt}-\left.\frac{du_b(x,t)}{dt}\right|_{x=vt}\right]+k_v\left[u_v(t)-\left.u_b(x,t)\right|_{x=vt}\right]=0 \tag{3}$$

where m_v, c_v and k_v are the mass, damping and stiffness of the vehicle, respectively; $u_v(t)$ is the vertical displacement of the vehicle; $\left.\frac{du_b(x,t)}{dt}\right|_{x=vt}$ denotes the vertical velocity of the bridge at the contact point $x=vt$, which can be further split up in terms of the vibration velocity of the bridge caused by the vehicle load and the additional vertical velocity of the wheel caused by the horizontal movement of the wheel along the slope of the bridge due to vibration on the right-hand side respectively as

$$\left.\frac{du_b(x,t)}{dt}\right|_{x=vt}=\left.\frac{\partial u_b(x,t)}{\partial t}\right|_{x=vt}+v\left.\frac{\partial u_b(x,t)}{\partial x}\right|_{x=vt} \tag{4}$$

Since in reality bridges are very stiff, the slope caused by the vehicle load is very small. Moreover, the vehicle speed is not very high. Therefore, the second term on the left-hand side of Equation (3) can be ignored, thereby giving

$$m_v\frac{d^2u_v(t)}{dt^2}+c_v\left[\frac{du_v(t)}{dt}-\left.\frac{\partial u_b(x,t)}{\partial t}\right|_{x=vt}\right]+k_v\left[u_v(t)-\left.u_b(x,t)\right|_{x=vt}\right]=0 \tag{5}$$

The contact force between the bridge and vehicle is

$$F_c(t)=-m_vg+k_v\left[u_v(t)-\left.u_b(x,t)\right|_{x=vt}\right]+c_v\left[\frac{du_v(t)}{dt}-\frac{\partial u_b(x,t)\big|_{x=vt}}{\partial t}\right] \tag{6}$$

The displacement of the bridge can be obtained as elaborated below.

Equation (1) is the equation of motion for the simply supported bridge and can be analyzed by mode superposition method [8]. The vertical displacement of bridge can be written as

$$u_b(x,t) = \sum_{i=1}^{\infty} \phi_i(x) Y_i(t) \tag{7}$$

where $\phi_i(x)$ is the ith mode shape of the bridge, and $Y_i(t)$ is the associated modal amplitude.

To evaluate the contribution of mode i to the bridge vertical displacement $u_b(x,t)$, substituting Equation (7) into Equation (1), multiplying both sides by $\phi_j(x)$ and integrating give

$$\begin{aligned} &\int_0^L \overline{m}\phi_j(x) \sum_{i=1}^{\infty} \left[\phi_i(x) \frac{d^2 Y_i(t)}{dt^2} \right] dx + \int_0^L c\phi_j(x) \sum_{i=1}^{\infty} \left[\phi_i(x) \frac{dY_i(t)}{dt} \right] dx + \\ &\int_0^L EI\phi_j(x) \sum_{i=1}^{\infty} \left[\frac{d^4 \phi_i(x)}{dx^4} Y_i(t) \right] dx = \int_0^L F_c(t) \delta(x - vt) \phi_j(x) dx \end{aligned} \tag{8}$$

Assuming the damping of the bridge to be Rayleigh damping which satisfies the orthogonality condition, and applying the orthogonality condition, i.e.

$$\left.\begin{array}{l} \phi_i(x) \cdot m \cdot \phi_j(x) \\ \phi_i(x) \cdot c \cdot \phi_j(x) \\ \phi_i(x) \cdot EI \cdot \phi_j(x) \end{array}\right\} = 0 \quad \textbf{if} \quad i \neq j \tag{9}$$

in Equation (8) yield

$$\begin{aligned} &\overline{m} \frac{d^2 Y_j(t)}{dt^2} \int_0^L \phi_j{}^2(x) dx + c \frac{dY_j(t)}{dt} \int_0^L \phi_j{}^2(x) dx + EI \cdot Y_j(t) \int_0^L \phi_j(x) \frac{d^4 \phi_j(x)}{dx^4} dx \\ &= F_c(t) \phi_j(x = vt) dx \end{aligned} \tag{10}$$

where only one term of each infinite series remains on the left hand side. Hence the amplitude term $Y_j(t)$ can be obtained by solving this ordinary differential equation.

The mode of a simply supported beam is of sinusoidal shape given by

$$\phi_j(x) = \sin \frac{j\pi x}{L} \tag{11}$$

Substituting Equations (6) and (11) into Equation (10), and rearranging yields

$$\begin{aligned} &\frac{d^2 Y_j(t)}{dt^2} + 2\xi_{bj}\omega_{bj} \frac{dY_j(t)}{dt} + \omega_{bj}^2 Y_j(t) = \frac{2}{\overline{m}L} \sin \frac{j\pi vt}{L} \times \\ &\left\{ -m_v g + m_v \omega_v \left[\omega_v u_v(t) + 2\xi_v \frac{du_v(t)}{dt} - \omega_v \sum_{k=1}^{\infty} \sin \frac{k\pi vt}{L} Y_k(t) - 2\xi_v \sum_{k=1}^{\infty} \sin \frac{k\pi vt}{L} \frac{dY_k(t)}{dt} \right] \right\} \end{aligned} \tag{12}$$

where ω_{bj} and ξ_{bj} are the jth frequency and damping-ratio of the bridge respectively, i.e.

$$\omega_{bj} = \frac{j^2 \pi^2}{L^2} \sqrt{\frac{EI}{\overline{m}}}, \quad \xi_{bj} = \frac{c}{2\overline{m}\omega_{bj}} \tag{13}$$

Assuming the vehicle mass to be negligible in comparison with the bridge mass, i.e. $\frac{m_v}{\overline{m}L} << 1$, the terms in square brackets on the right-hand side of Equation (12) can be ignored, giving

$$\frac{d^2Y_j(t)}{dt^2} + 2\xi_{bj}\omega_{bj}\frac{dY_j(t)}{dt} + \omega_{bj}^2 Y_j(t) = \frac{-2m_v g}{\overline{m}L}\sin\frac{j\pi vt}{L} \tag{14}$$

Solving Equation (14) yields a solution for the modal amplitude $Y_j(t)$ as

$$\begin{aligned} Y_j(t) &= (M\cos\omega_{bjd}t + N\sin\omega_{bjd}t)^{-\xi_{bj}\omega_{bj}t} + \\ &\frac{\Delta_{bj}}{(1-\beta_j^2)^2 + (2\xi_{bj}\beta_j)^2}\left[(1-\beta_j^2)\sin\frac{j\pi vt}{L} - 2\xi_{bj}\beta_j\cos\frac{j\pi vt}{L}\right] \end{aligned} \tag{15}$$

where the constants M and N can be evaluated for any given initial conditions, $Y_j(0)$ and $\left.\frac{dY_j(t)}{dt}\right|_{t=0}$, the first term on the right-hand side accounts for the transient response that will damp out exponentially, and the second term represents the steady state harmonic response that will continue indefinitely. However, since the transient response damps out quickly, it is not the primary concern. Here the solutions under the initial condition $Y_j(0) = 0$ and $\left.\frac{dY_j(t)}{dt}\right|_{t=0} = 0$ are provided as an example. The *j*th frequency of the damped bridge ω_{bjd}, the static vertical displacement of the *j*th mode caused by the vehicle loading Δ_{bj}, the dimensionless speed parameter β_j, and constants M and N are given as follows

$$\omega_{bjd} = \omega_{bj}\sqrt{1-\xi_{bj}^2} \tag{16}$$

$$\Delta_{bj} = \frac{-2m_v gL^3}{j^4\pi^4 EI} \tag{17}$$

$$\beta_j = \frac{j\pi v}{L\omega_{bj}} \tag{18}$$

$$M = \frac{2\xi_{bj}\beta_j\Delta_{bj}}{(1-\beta_j^2)^2 + (2\xi_{bj}\beta_j)^2} \tag{19}$$

$$N = \frac{\Delta_{bj}}{(1-\beta_j^2)^2 + (2\xi_{bj}\beta_j)^2}\left[\frac{2j\pi\xi_{bj}\beta_j v - (1-\beta_j^2)\xi_{bj}\omega_{bj}L}{\omega_{bjd}L}\right] \tag{20}$$

Ignoring the transient responses in Equation (15) and substituting it into Equation (7), the vertical displacement of bridge can be obtained as

$$u_b(x,t) = \sum_{j=1}^{\infty}\frac{\Delta_{bj}}{(1-\beta_j^2)^2 + (2\xi_{bj}\beta_j)^2}\left[(1-\beta_j^2)\sin\frac{j\pi vt}{L} - 2\xi_{bj}\beta_j\cos\frac{j\pi vt}{L}\right]\sin\frac{j\pi x}{L} \tag{21}$$

Differentiating Equation (21) with respect to time t, the vertical velocity of the bridge is obtained as

$$\frac{\partial u_b(x,t)}{\partial t}=\sum_{j=1}^{\infty}\frac{\Delta_{bj}}{(1-\beta_j^2)^2+(2\xi_{bj}\beta_j)^2}\frac{j\pi v}{L}\left[(1-\beta_j^2)\cos\frac{j\pi vt}{L}+2\xi_{bj}\beta_j\sin\frac{j\pi vt}{L}\right]\sin\frac{j\pi x}{L} \quad (22)$$

Hence Equation (21) and (22) indicate that the vertical displacement as well as velocity of the bridge are linearly related to the mass of vehicle m_v.

2.2 2.2 Vehicle-bridge interaction model with surface roughness

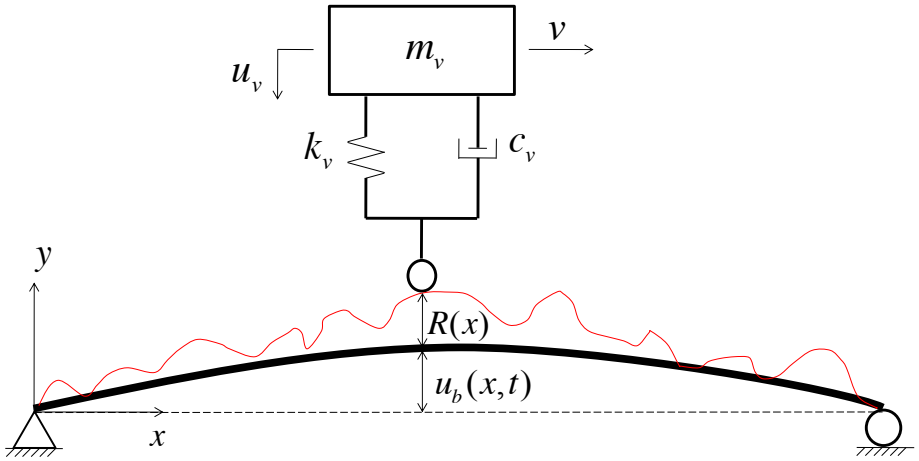

Figure 2 Vehicle-bridge interaction model with surface roughness

Two assumptions are made to establish the vehicle-bridge interaction model with surface roughness as shown in Figure 2. The wheel of the vehicle is always in contact with the bridge surface, i.e. the vehicle does not bounce on the bridge. The surface roughness profile remains unchanged during multiple passes in a short period.

Based on these two assumptions, the vertical displacement of the wheel of vehicle is equal to the sum of the vertical displacement of the bridge at the contact point and the surface roughness, i.e.

$$u_w(t)=u_b(x,t)\big|_{x=vt}+R(vt) \quad (23)$$

where $u_w(t)$ is the vertical displacement of the vehicle wheel, and $R(vt)$ is the surface roughness at the contact point $x=vt$. With the surface roughness taken into consideration, $u_b(x,t)\big|_{x=vt}$ in Equation (3) should be replaced by $u_w(t)$ in Equation (23), which yields

$$m_v\frac{d^2u_v(t)}{dt^2}+c_v\left\{\frac{du_v(t)}{dt}-\frac{d\left[u_b(x,t)\big|_{x=vt}+R(vt)\right]}{dt}\right\}+k_v\left\{u_v(t)-\left[u_b(x,t)\big|_{x=vt}+R(vt)\right]\right\}=0 \quad (24)$$

Substituting Equation (4) into Equation (24) and ignoring the additional vertical velocity of the wheel yields

$$m_v\frac{d^2u_v(t)}{dt^2}+c_v\frac{du_v(t)}{dt}+k_vu_v(t)=c_v\frac{\partial u_b(x,t)}{\partial t}\bigg|_{x=vt}+k_vu_b(x,t)\big|_{x=vt}+vc_v\frac{dR(vt)}{d(vt)}+k_vR(vt) \quad (25)$$

which is the equation of motion of the vehicle considering the effect of surface roughness.

2.3 Method for estimation of surface roughness profile

Based on Equation (25), a double-pass mass-addition technique is proposed to estimate the bridge surface roughness profile, as elaborated below.

Step 1: Let the test vehicle of mass m_v with accelerometer installed on it move on the bridge at a constant speed v, and record its vertical acceleration response history $a_1(t)$.

Step 2: Add a certain mass on the vehicle so that the total vehicle mass becomes λm_v where λ is a parameter slightly above unity, e.g. 1.1. Let the vehicle with added mass move on the bridge once more at the same speed v, and record its vertical acceleration response history $a_2(t)$.

Step 3: Calculate the following two time series ans_1 and ans_2 which are derived from Equation (25):

$$\begin{aligned} ans_1 &= c_v \left.\frac{\partial u_b(x,t)}{\partial t}\right|_{x=vt} + k_v u_b(x,t)\big|_{x=vt} + vc_v \frac{dR(vt)}{d(vt)} + k_v R(vt) \\ &= m_v a_1(t) + c_v v_1(t) + k_v u_1(t) \end{aligned} \tag{26}$$

$$\begin{aligned} ans_2 &= \lambda c_v \left.\frac{\partial u_b(x,t)}{\partial t}\right|_{x=vt} + \lambda k_v u_b(x,t)\big|_{x=vt} + vc_v \frac{dR(vt)}{d(vt)} + k_v R(vt) \\ &= \lambda m_v a_2(t) + c_v v_2(t) + k_v u_2(t) \end{aligned} \tag{27}$$

where $u_1(t)$ and $u_2(t)$ are the vertical displacement histories of the vehicle in the first and second passes respectively, $v_1(t)$ and $v_2(t)$ are the vertical velocity histories of the vehicle in the first and second passes respectively, which can be obtained by numerical integration of the acceleration histories $a_1(t)$ and $a_2(t)$.

Combining Equations (26) and (27) yields

$$vc_v \frac{dR(vt)}{d(vt)} + k_v R(vt) = ans_1 - \frac{1}{\lambda - 1}(ans_2 - ans_1) \tag{28}$$

which is an ordinary differential equation involving the surface roughness $R(vt)$, which can be solved numerically by methods such as Euler method or Runge–Kutta methods.

2.4 Differentiability of the surface roughness

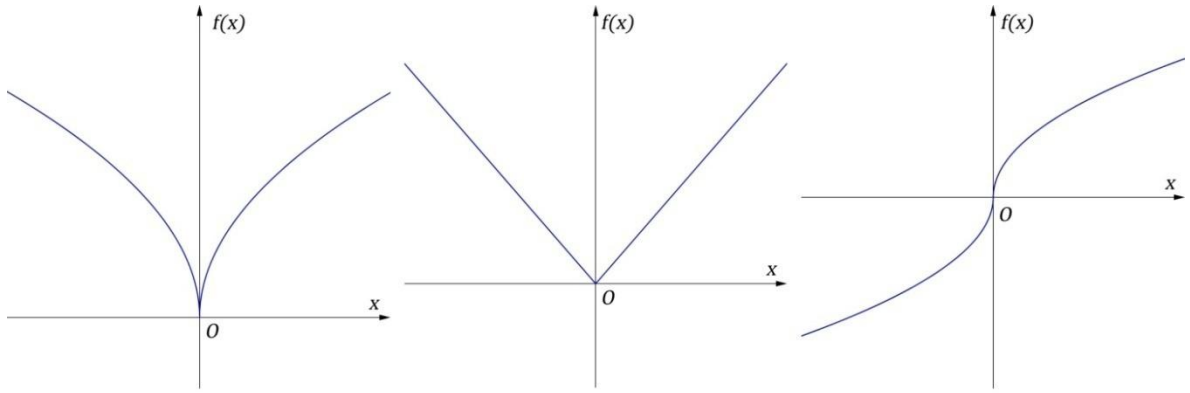

(a) Cusp at x = 0 (b) Corner at x = 0 (c) Vertical tangent at x = 0

Figure 3 Possible non-differentiable cases in surface roughness profile

In reality, the surface roughness can be of any shape. If it is described mathematically as a function of abscissa x, it might not be differentiable for any x. The surface roughness must be continuous without any removable or jump discontinuity, but in theory it could have vertical tangent points, corners and/or cusps, which make these points non-differentiable, as shown in Figure 3. This means that the transformation from Equation (23) to Equation (24) is not always mathematically feasible. However, the surface roughness is treated as a series of discrete points instead of a continuous curve in engineering. The interval between adjacent points is decided by the sampling rate or distance. The derivatives of series of discrete points can be obtained numerically, and therefore the differentiability of the surface roughness has no effect on the applicability of this method.

3 NUMERICAL VERIFICATION

The feasibility of the proposed method is verified numerically with different classes of surface roughness profile. Two error indicators are introduced to evaluate the performance of this method.

3.1 Generation of surface roughness for simulation

The standard ISO 8608 *Mechanical Vibration-Road Surface Profiles-Reporting of Measured Data* [9] classifies the surface profile into 5 categories based on their power spectral density and provides the following process to generate surface roughness for simulation purpose.

It is a commonly assumed hypothesis that the randomness of the road surface roughness can be represented by a normal zero-mean, real-valued stationary Gaussian process as

$$R(x)=\sum_{i=0}^{N}\sqrt{2G_d(n_i)\Delta n}\cos(2\pi n_i x+\phi_i) \tag{29}$$

where N is the total number of harmonic waves used to construct the roughness profile, which usually varies from a few hundred to a few thousand; ϕ_i is the random phase angle uniformly distributed in the interval [0, 2π] (inclusive); and $G_d(n_i)$, Δn and n_i are defined as follows

$$G_d(n_i)=G_d(n_0)\left(\frac{n_i}{n_0}\right)^{-w} \tag{30}$$

$$\Delta n=\frac{n_u-n_l}{N} \tag{31}$$

$$n_i=n_l+i\Delta n \tag{32}$$

in which n_u and n_l are the upper and lower spatial frequency limits taken as 0.01 m^{-1} and 10 m^{-1} respectively, the reference spatial frequency n_0 is taken as 0.1 m^{-1}, the exponent is taken as $w=2$, and the parameter $G_d(n_0)$ is determined based on the roughness class as shown in Table 1 according to the ISO standard [9].

To verify the effectiveness and applicability of the proposed method, three sets of surface roughness profile belonging to classes A, C and E are generated. The total number of sinusoidal wave used to form the roughness profile N is taken as 1024. The generated surface roughness profile are shown in Figure 4 to Figure 6 respectively.

Road class	Description	$G_d(n_0)$ (10^{-6}m^3)		
		Lower limit	Geometric mean	Upper limit
A	Very good	--	16	32
B	Good	32	64	128
C	Average	128	256	512
D	Poor	512	1024	2048
E	Very poor	2048	4096	8192

Table 1 Parameter $G_d(n_0)$ for different road classes

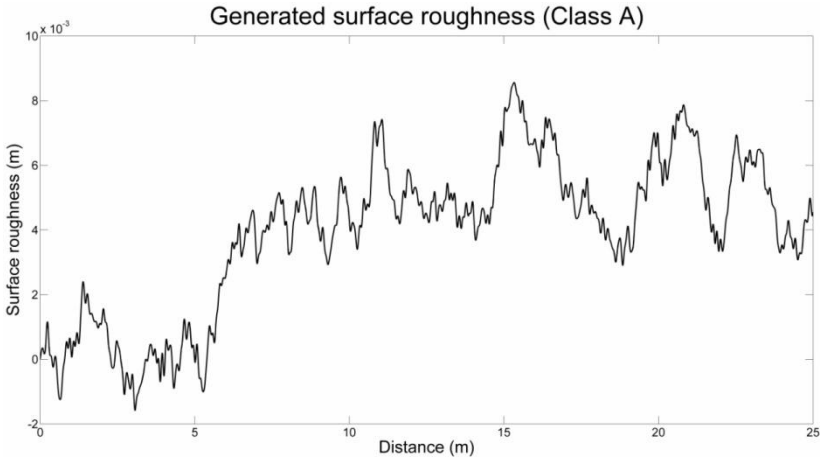

Figure 4 Generated surface roughness (Class A: Very good)

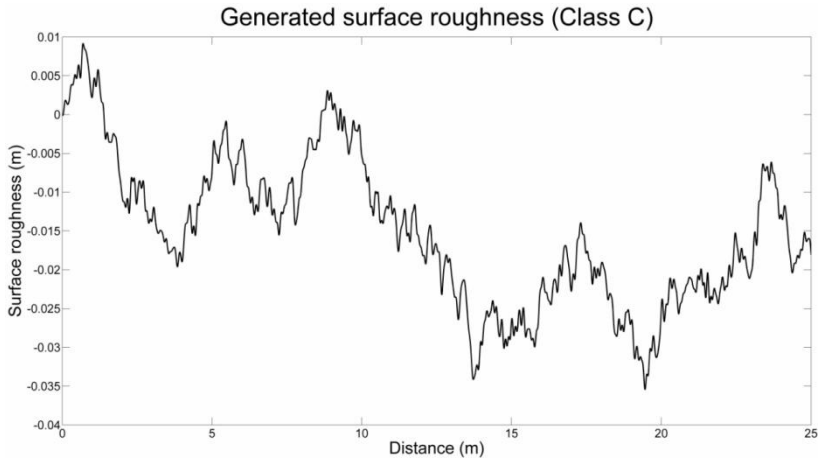

Figure 5 Generated surface roughness (Class C: Average)

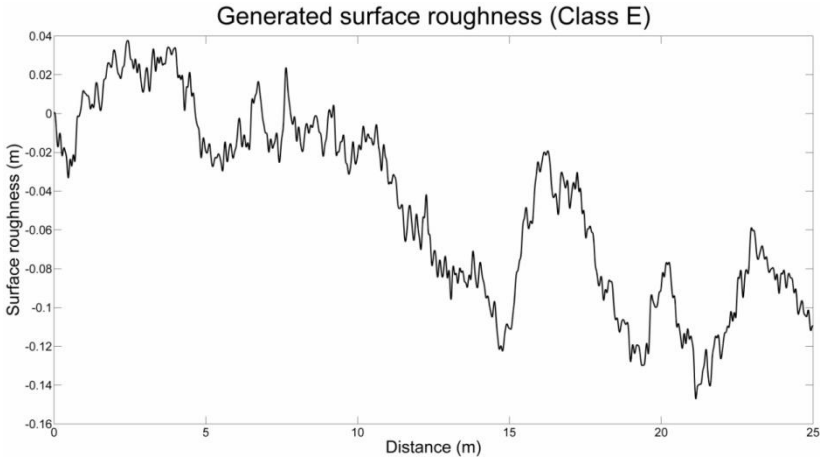

Figure 6 Generated surface roughness (Class E: Very poor)

3.2 Error indicator

To better evaluate the effectiveness of the proposed method, two error indicators, emphasizing on the absolute and relative errors respectively, are introduced.

Minkowski distance can be used to measure the difference between two series, i.e.

$$err_1 = \left(\sum_{i=1}^{n} |a_i - b_i|^p \right)^{\frac{1}{p}} \tag{33}$$

where $p > 1$. Here we adopt the most commonly used Minkowski distance with p being 2, which is also known as the Euclidean distance. It is the distance between two points in Euclidean n-space, which can be used to measure the difference between two series. This indicator omits the absolute values of the two series and only focuses on their absolute difference. It has also an accumulative nature, and hence it cannot decrease as more terms are used in the series.

Since Minkowski distance cannot effectively measure the relative similarity of two series, the relative area difference is introduced, as

$$err_2 = \frac{\int |a(x) - b(x)| \, dx}{\int |b(x)| \, dx} \tag{34}$$

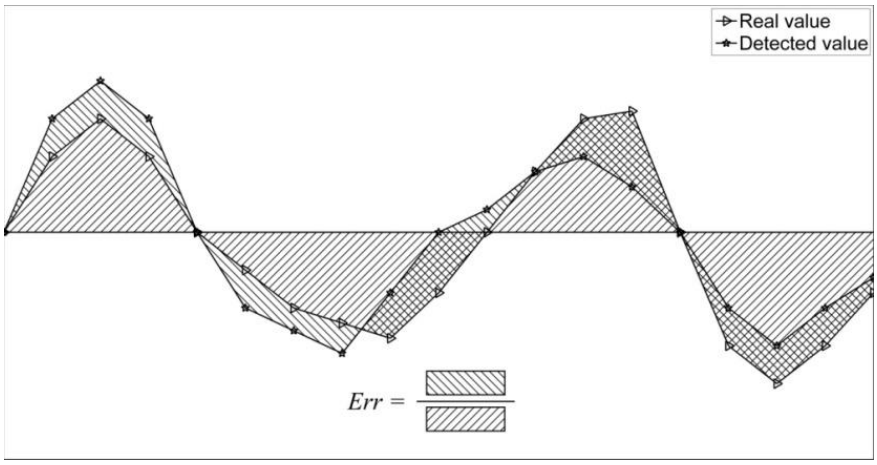

Figure 7 Relative area difference

Equation (34) can be construed as the ratio of the area between the detected value and the real value to the area of the real value as illustrated in Figure 7. This indicator takes the relative relationship between the detection error and the real value into account. Therefore, if the variation of the real value itself is higher, then the same relative area difference means a higher tolerance for the detected value.

3.3 Finite element simulation

The vehicle and bridge parameters used in the finite element simulation can be found in Table 2 and Table 3.

Mass (kg)	Stiffness ($N \cdot m^{-1}$)	Damping ($N \cdot s \cdot m^{-1}$)	Speed ($m \cdot s^{-1}$)	Sampling Frequency (s^{-1})	Added mass (kg)	Add mass ration λ
1000	5×10^4	5000	10	1000	100	1.1

Table 2: Vehicle parameters for FE modeling

Span (m)	EI ($N \cdot m^2$)	Mass ($kg \cdot m^{-1}$)	Damping ratio		Element number
			1st mode	2nd mode	
25	3.3×10^9	4800	0.02	0.02	25

Table 3 Bridge parameters for FE modeling

The simulation results for different surface roughness classes are shown in Table 4 and Figure 8 to Figure 10.

Surface roughness class	err_1 (10^{-3}m)	err_2 (%)
A	1.3×10^{-3}	0.49
C	4.8×10^{-3}	0.45
E	16.7×10^{-3}	0.46

Table 4 Results of error indicators

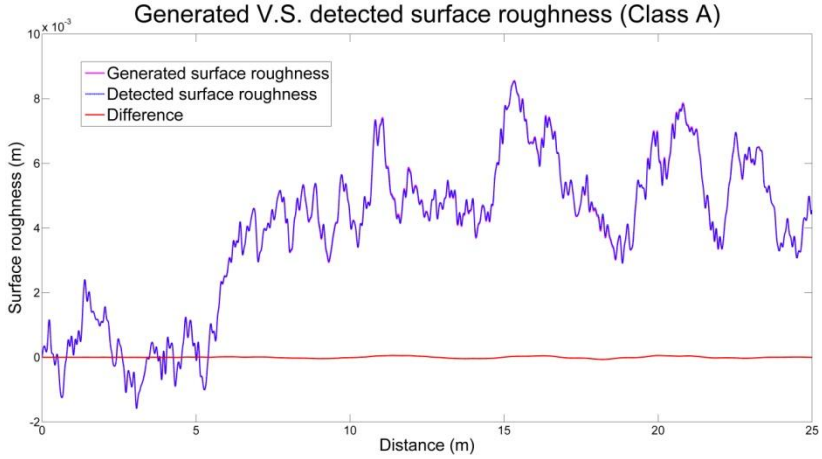

Figure 8 Surface roughness detection results (Class A: Very good)

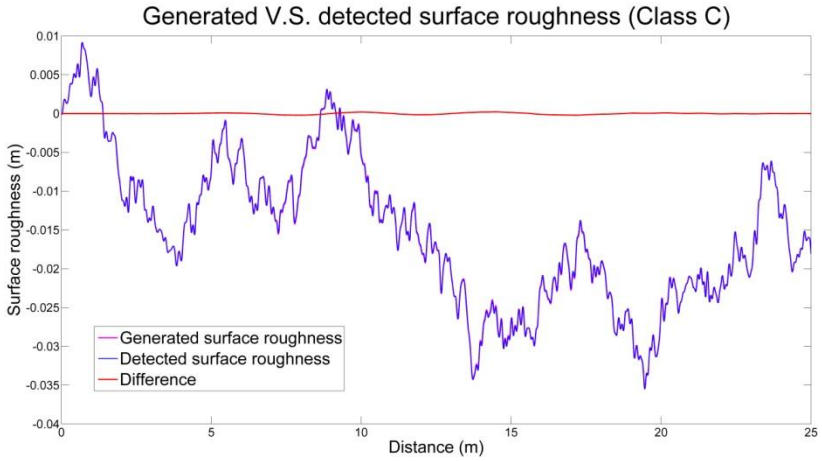

Figure 9 Surface roughness detection results (Class C: Average)

It can be concluded, both visually and based on the error indicators, that the simulation results are of satisfactory accuracy. The variation between the detected and generated surface roughness is very small compared to the variation of the generated surface roughness itself. As the variation of the generated surface roughness increases (the surface class becomes worse), the absolute detection error represented by err_1 also increases, but the relatively error represented by err_2 stays almost the same. Therefore, this method can be considered as effective for most bridges, whether their surface conditions are good or poor.

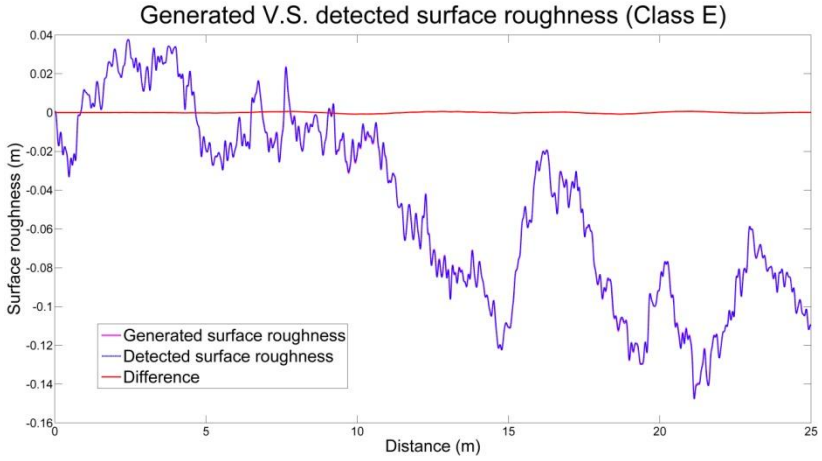

Figure 10 Surface roughness detection results (Class E: Very poor)

3.4 Discussion of errors

The error between the detected and generated surface roughness may be caused by various simplifying assumptions. Assuming the vehicle mass to be negligible in comparison with the bridge mass leads to several terms in Equation (12) being neglected. Ignoring the transient responses simplifies Equation (15) significantly but also introducing errors. The responses of the vehicle-bridge system obtained do not satisfy the governing equations exactly. The assumption of linear relationship between the bridge response and vehicle mass may also introduce some error. Further improvement can be achieved by boosting the accuracy of responses through iteration. Moreover, using numerical integration to calculate $u_v(t)$ and $v_v(t)$ from

$a_v(t)$ and the numerical solution of differential equations will inevitably cause a loss of accuracy.

4 CONCLUSION

In order to estimate the surface roughness of a bridge, this study presents a double-pass mass-addition method. The information required by this method includes the acceleration response histories extracted from an instrumented vehicle equipped with an accelerometer running on the bridge twice, with an added mass in the second time. Numerical simulation proves that this method is able to estimate the bridge surface roughness with satisfactory accuracy regardless of its surface quality.

This method is useful in reducing the uncertainties associated with surface roughness in vehicle bridge interaction and improving the accuracy of numerical simulation, which are helpful to the drive-by bridge parameter identification.

In order to get results with satisfactory accuracy, one should be mindful of the basic assumptions. The test vehicle should not be too heavy compared to the bridge mass, and the vehicle should not be too fast to avoid any loss of contact with the bridge.

ACKONWLEDGEMENTS

The authors acknowledge financial support from the Hong Kong PhD Fellowship Scheme of the Hong Kong Research Grants Council for the first author.

REFERENCES

[1] F.T.K. Au, R.J. Jiang, Y.K. Cheung, Parameter identification of vehicles moving on continuous bridges. *Journal of sound and vibration*, **269**, 91-111, 2004.

[2] Y.B. Yang, C.W. Lin, Vehicle–bridge interaction dynamics and potential applications. *Journal of sound and vibration*, **284**, 205-226, 2005.

[3] A. González, E.J. O'Brien, P. McGetrick, Identification of damping in a bridge using a moving instrumented vehicle. *Journal of Sound and Vibration*, **331**, 4115-4131, 2012.

[4] Z.H. Li, F.T.K. Au, Damage detection of a continuous bridge from response of a moving vehicle. *Shock and Vibration*, 2014.

[5] K.V. Nguyen, Comparison studies of open and breathing crack detections of a beam-like bridge subjected to a moving vehicle. *Engineering Structures*, **51**, 306-314, 2013.

[6] Y.B. Yang, Y.C. Li, K.C. Chang, Constructing the mode shapes of a bridge from a passing vehicle: a theoretical study. *Smart Structures and Systems*, **13**, 797-819, 2014.

[7] C.W. Kim, M. Kawatani, J. Hao, Modal parameter identification of short span bridges under a moving vehicle by means of multivariate AR model. *Structure and Infrastructure Engineering*, **8**, 459-472, 2012.

[8] R.W. Clough, J. Penzien, *Dynamics of Structures*. Computers & Structures Inc., 1995.

[9] ISO, ISO8608 *Mechanical vibration-Road surface profiles-Reporting of measured data*. International Organization for Standardization (ISO) Geneva, 1995.